RESEARCH ARTICLE

Screening for the anti-gastric cancer activity of traditional Chinese medicine components using a dual-model system of gastric cancer cells and organoids

Lingxian Tong[1], Zhihui Xu[1,2], Yingqiu Pan[3], Jun Li[3], Hunli Xia[3], Lijuan Zhai[2], Xiang Wang[2], Jian Ge[1,*]

[1]College of Life Sciences, China Jiliang University, Hangzhou, Zhejiang, China. [2]Hangzhou Youdu Biotechnology Co., Ltd., Hangzhou, Zhejiang, China. [3]Taizhou Food and Drug Inspection and Research institute, Taizhou, Zhejiang, China.

Received: May 21, 2026; **accepted:** September 23, 2026.

Gastric cancer (GC) remains a high-mortality malignancy, while conventional two-dimensional cell models poorly recapitulate tumor heterogeneity, causing unreliable preclinical drug screening results. Chinese herbal monomers (CHMs) exhibit favorable anti-tumor properties with low toxicity, and patient-derived gastric cancer organoids (GCOs) better simulate clinical tumor characteristics. However, systematic evaluation of CHM anti-GC effects using a dual-model system integrating cell lines and patient-derived organoids remains limited. This study screened active anti-GC CHMs using a dual-model system, investigated the molecular mechanism of key compounds, and evaluated the utility of GCOs for drug sensitivity assessment. Eight CHMs were preliminarily screened in three GC cell lines of AGS, SGC-7901, and BGC-823. Cell proliferation and apoptosis were detected using the Cell Counting Kit-8 (CCK-8) assays and flow cytometry. A GCO library was established. CHM drug sensitivity was assessed by CellTiter-Lumi™ and apoptosis using Annexin V–fluorescein isothiocyanate (Annexin V-FITC)/7-aminoactinomycin D (7-AAD) staining. Western blotting was performed to examine apoptosis-related proteins and PI3K/AKT pathway. The results showed that curcumin, berberine, and ursolic acid exerted prominent anti-tumor effects. The three GCO lines exhibited heterogeneous drug responses with GC-34 showing the highest sensitivity, particularly to ursolic acid compared with the clinical chemotherapeutic 5-fluorouracil. Mechanistically, ursolic acid induced GC apoptosis by upregulating Cleaved-caspase-3 and Bax, downregulating Bcl-2, and suppressing the PI3K/AKT pathway *via* reduced p-PI3K, p-AKT, and P53 expression ($P < 0.05$). The findings supported the utility of the dual-model system for anti-GC drug screening, verified the application value of GCOs, and provided solid experimental evidence for the clinical translational potential of ursolic acid and related CHMs in GC treatment.

Keywords: gastric cancer; patient-derived organoids; Chinese herbal monomers; ursolic acid; apoptosis; PI3K/AKT signaling pathway.

[*]**Corresponding author:** Jian Ge, College of Life Sciences, China Jiliang University, Hangzhou, Zhejiang 310018, China. Email: gejian@cjlu.edu.cn.

Introduction

Gastric cancer (GC) is one of the most common malignancies of the digestive system with more than one million new cases diagnosed annually worldwide [1]. Despite a gradual decline in its incidence and mortality over the past several decades, GC remains the fifth most frequently diagnosed cancer and the third leading cause of cancer-related death worldwide [2]. The development of GC is closely associated with multiple risk factors including *Helicobacter pylori* and Epstein–Barr virus infection, genetic predisposition [3], smoking, and unhealthy

dietary habits [4]. Although considerable progress has been achieved in the prevention, diagnosis, and treatment of GC [5], the prognosis of patients with advanced GC remains unsatisfactory because of tumor heterogeneity, therapeutic resistance, and late-stage diagnosis. Therefore, identifying novel and effective therapeutic agents remains an urgent clinical challenge to improve patient survival and quality of life [6].

Traditional Chinese medicine (TCM) has attracted increasing attention as a promising source of anti-cancer therapeutics [7]. Numerous studies have demonstrated that active components of Chinese herbal medicines (CHMs) possess multiple pharmacological activities including enhancing therapeutic efficacy [8], reducing treatment-related toxicity [9], overcoming drug resistance, and improving patient prognosis [10]. These characteristics suggest that CHMs have considerable potential as complementary or alternative therapeutic agents for GC [11]. However, the successful translation of promising CHMs into clinical applications depends on reliable preclinical models capable of accurately predicting therapeutic responses. Conventional two-dimensional (2D) cancer cell models are widely used for anti-cancer drug screening because of their simplicity, accessibility, and scalability [12]. However, these models cannot faithfully reproduce the three-dimensional architecture, cellular heterogeneity, and tumor microenvironment of human cancers, thereby limiting their predictive value for clinical efficacy [13]. Recently, patient-derived organoid technology has emerged as an advanced three-dimensional culture system that preserves the histopathological characteristics, genetic alterations, and biological heterogeneity of primary tumors [14]. Gastric cancer organoids (GCOs) established from patients with different histological subtypes and clinical stages have shown great promise for disease modeling [15], personalized medicine, and preclinical drug screening [16]. Despite these advances, systematic evaluation of CHM-derived compounds across conventional GC cell lines and patient-derived GCOs remains limited [17]. Consequently, the anti-cancer potential of many CHMs has not been comprehensively validated, and the feasibility of GCOs as a platform for evaluating the efficacy of Chinese herbal compounds remains insufficiently explored. Moreover, the molecular mechanisms underlying the anti-tumor effects of promising CHMs in GCOs have yet to be fully elucidated. Addressing these issues is essential for accelerating the discovery and clinical translation of novel anti-GC agents derived from TCM [10, 17].

This study aimed to systematically screen CHMs with anti-GC activity using both GC cell lines and patient-derived GCOs to identify candidate compounds with potent anti-tumor effects and investigate their underlying molecular mechanisms. Eight representative CHMs were first screened in three GC cell lines using cell proliferation and apoptosis assays. Candidate compounds were subsequently evaluated in a patient-derived GCO library by assessing cell viability and apoptosis followed by Western blot analysis to investigate apoptosis-related proteins and the PI3K/AKT signaling pathway. This study established a dual-model screening system integrating conventional GC cell lines with patient-derived organoids for evaluating anti-GC compounds from TCM. The findings not only provided experimental evidence supporting the reliability and applicability of GCOs for preclinical drug sensitivity assessment, but also offered new insights into the molecular mechanisms of active CHMs and provided a scientific basis for the further development and clinical translation of ursolic acid and other promising CHMs in GC therapy.

Materials and methods

Clinical sample collection and establishment of patient-derived GCOs

Tumor tissue samples were collected from 20 patients with gastric adenocarcinoma who underwent surgical resection at the Department of Pancreatic and Gastric Surgery of Ningbo No. 2

Hospital (Ningbo, Zhejiang, China) between March 2023 and August 2024. The diagnosis was confirmed by pathological examination, and relevant clinical information was recorded. The inclusion criteria were age > 18 years, an Eastern Cooperative Oncology Group performance status (ECOG PS) score of ≤ 2 and eligible for radical gastrectomy, the presence of a single primary gastric tumor without distant metastasis, and the absence of other severe comorbidities that could affect the study outcomes. All procedures of this research were approved by the Medical Ethics Committee of Ningbo No. 2 Hospital (Ningbo, Zhejiang, China) with the approval number of YJ-KYSB-NBEY-2019-105-01. Written informed consents were obtained from all patients prior to sample collection. Patient-derived GCOs were established from freshly resected gastric tumor tissues. The established organoid lines were designated according to their corresponding sample identifiers with GC-32, GC-34, and GC-47 representing three independent GCO lines derived from three different patients with gastric adenocarcinoma. These three organoid lines were selected for subsequent drug-response and mechanistic experiments.

Preparation of stock solutions of traditional Chinese medicine-derived compounds

All procedures were performed under sterile conditions. Resveratrol, curcumin, kaempferol, baicalein, berberine, erianin, quercetin, and ursolic acid were obtained from Shanghai Yuanye Bio-Technology Co., Ltd. (Shanghai, China). For each compound, 20 mg was accurately weighed and dissolved in an appropriate volume of cell culture-grade dimethyl sulfoxide (DMSO) (Beijing Solarbio Science & Technology Co., Ltd., Beijing, China) to obtain the desired stock concentration with the required DMSO volume calculated according to the molecular weight and target concentration of each compound. The final stock concentrations of erianin, baicalein, kaempferol, berberine, resveratrol, curcumin, ursolic acid, and quercetin were 40, 160, 100, 100, 120, 60, 70, and 200 mM, respectively. For compounds with limited solubility, ultrasound-assisted dissolution was performed using AS3120 ultrasonic cleaner (Hangzhou Micronpai Technology Co., Ltd., Hangzhou, Zhejiang, China) at 37°C and 40 kHz for 1 min. After complete dissolution, the stock solutions were aliquoted into sterile polymerase chain reaction (PCR) tubes and stored at −20°C.

Cells and cell culture

Human GC cell lines AGS (BNCC33814), BGC-823 (BNCC352070), and SGC-7901 (BNCC100674) were obtained from Benna Biotechnology Co., Ltd. (Hangzhou, Zhejiang, China). AGS cells were cultured in DMEM/F-12 medium, while BGC-823 cells were cultured in high-glucose DMEM (DMEM-H), and SGC-7901 cells were cultured in RPMI-1640 medium. All media were provided by Tianjin Haoyang Biological Products Technology Co., Ltd., Tianjin, China and supplemented with 10% fetal bovine serum (FBS) (ExCell Bio, Suzhou, Jiangsu, China) and 1% penicillin–streptomycin. Cells were maintained in HF90 humidified CO_2 incubator (Shanghai Lishen Scientific Equipment Co., Ltd., Shanghai, China) at 37°C with 5% CO_2. Cell morphology and confluence were monitored daily, and the culture medium was replaced regularly to maintain appropriate cell growth and confluence.

Drug treatment and viability assessment of patient-derived GCOs

Based on the preliminary screening of the eight CHM-derived compounds in AGS, SGC-7901, and BGC-823 cells, curcumin, berberine, and ursolic acid were selected for subsequent evaluation in the patient-derived GCO models. According to the Guidelines for the Diagnosis and Treatment of Gastric Cancer (2022), 5-fluorouracil (5-FU) was selected as the positive-control drug [6]. GCOs were treated with berberine at 12.5, 25, 35, 50, and 70 μM; curcumin at 40, 60, 80, 100, and 120 μM; ursolic acid at 7.5, 10, 15, 20, and 30 μM; and 5-FU at 50, 75, 100, 150, and 200 μM, respectively. Following continuous treatment for 120 h, morphological changes were examined by bright-field microscopy. Organoid viability was quantitatively assessed using the CellTiter-Lumi™ 3D luminescent cell viability assay (Biotime Biotechnology, Shanghai, China) according to the

manufacturer's instructions. Dose–response curves were generated based on viability data, and the half-maximal inhibitory concentration (IC_{50}) values were calculated by nonlinear regression analysis.

Cell viability assay

Cell viability was assessed using a Cell Counting Kit-8 (CCK-8) (Vazyme Biotech Co., Ltd., Nanjing, Jiangsu, China). Log-phase GC cells were collected, counted, and resuspended at a density of 5×10^4 cells/mL. The cells were seeded into 96-well plates at 200 µL per well and incubated in a humidified CO_2 incubator at 37°C with 5% CO_2 to allow cell attachment. After cell attachment, the cells were treated with different concentrations of the eight CHM-derived compounds. The tested concentrations were resveratrol at 40, 50, 60, 70, 80, and 100 µM; curcumin at 10, 15, 20, 25, 30, 40, and 50 µM; kaempferol at 25, 30, 50, 60, 80, 100, and 150 µM; baicalein at 10, 20, 40, 60, 80, 120, and 160 µM; berberine at 12.5, 25, 35, 50, and 70 µM; erianin at 10, 20, 30, and 40 nM; quercetin at 60, 80, 100, 120, 160, 200, and 300 µM; and ursolic acid at 5, 10, 12.5, 15, and 35 µM. Cells treated with 0.1% DMSO served as the vehicle-control group, whereas wells containing CCK-8 working solution without cells served as the blank group. Each treatment group was tested in six technical replicate wells, and independent wells were designated for the 24, 48, and 72 h treatment groups. After the respective treatment period, the culture medium was removed, and the cells were washed with phosphate-buffered saline (PBS). 100 µL of CCK-8 working solution was added to each well, and the cells were incubated for 1 – 2 h before measurement. Absorbance at 450 nm was measured using SpectraMax Mini multifunctional microplate reader (Molecular Devices, San Jose, CA, USA). The experiment was independently repeated three times. Cell viability was calculated from the absorbance values (OD) as follows.

$$\text{Cell viability (\%)} = [(As - Ab) / (Ac - Ab)] \times 100\% \quad (1)$$

where As, Ab, and Ac were the OD values of the experimental group, blank group, and control group, respectively.

Colony formation assay

Log-phase cells were trypsinized and resuspended to obtain a single-cell suspension. The cell suspension was centrifuged at 1,300 rpm for 3 min, resuspended, and counted. AGS cells were seeded at 800 cells/well into 6-well plates with 2 mL per well, while SGC-7901/BGC-823 cells were seeded at 1,000 cells/well. After gentle mixing, the plates were incubated in the humidified CO_2 incubator at 37°C with 5% CO_2 for 24 h. After cell attachment, the cells were divided into experimental and vehicle-control groups. The experimental groups were treated with resveratrol at 15 and 30 µM; curcumin at 7.5 and 15 µM; kaempferol at 15 and 30 µM; baicalein at 10 and 20 µM; berberine at 5 and 10 µM; erianin at 10 and 20 nM; quercetin at 40 and 60 µM; and ursolic acid at 1.75 and 3.5 µM. The vehicle-control group received complete culture medium containing 0.1% DMSO. The culture medium was replaced every 5 - 7 days, and the cells were maintained for 12 - 14 days until visible colonies formed. The medium was then removed, and the cells were washed with PBS and fixed with 4% paraformaldehyde for 30 - 60 min. The fixed colonies were subsequently stained with crystal violet for 30 min in the dark, washed with PBS, air-dried, and photographed. Colony counts were performed using ImageJ (https://imagej.net/ij/). The experiment was repeated three times, and the colony formation rate was calculated as follows.

$$\text{Colony formation rate} = (\text{No. of colonies} / \text{No. of seeded cells}) \times 100\% \quad (2)$$

Flow cytometry

Apoptosis was assessed using Annexin V-FITC/7-AAD staining. AGS, SGC-7901, and BGC-823 cells were collected after incubation with different concentrations of drugs for 24 h, which were then washed twice with PBS and once with flow cytometry sample buffer followed by resuspension in 6 µL AnnexinV-FITC and 3 µL

propidium iodide (PI) in pre-cooled 1× binding buffer. These cells were incubated at room temperature in the dark for 5 - 10 min. Apoptosis was analyzed using FongCyte™ 2, two-laser, six-color system flow cytometer (Beijing Challen Biotechnology Co., Ltd., Beijing, China) by detecting Annexin V–FITC and PI fluorescence in separate channels to distinguish viable, early apoptotic, late apoptotic, and necrotic cells. The experiment was independently repeated three times, and the data were analyzed using FlowJo software (version 10.8.1) (BD Life Sciences, Ashland, OR, USA).

Culture and preparation of patient-derived GCOs for drug screening

GC organoids were cultured and passaged according to established protocols. When most organoids reached a diameter of approximately 200 – 300 μm, organoids were passaged at a 1:1.5 splitting ratio. Briefly, the culture medium was removed, and 1 mL of pre-chilled organoid buffer was added to each well. The Matrigel droplets containing organoids were gently dissociated by repeated pipetting and transferred into 15 mL centrifuge tubes. The samples were incubated at −20°C for 3 – 5 min and gently mixed to facilitate Matrigel dissolution and organoid separation. The organoids were collected by centrifugation at 1,650 rpm for 5 min at 4°C. The collected organoid pellets were resuspended in organoid passage digestion solution (Biorigin Biotechnology Co., Ltd., Beijing, China) and gently pipetted for 1 – 2 min to achieve appropriate digestion while avoiding excessive disruption. Digestion was terminated by adding 3 – 4 volumes of organoid buffer followed by centrifugation at 1,650 rpm for 5 min at 4°C. After removing the supernatant, the organoid pellets were resuspended in pre-chilled Matrigel (Quanxin QuanYi Life Science and Technology Co., Ltd., Shanghai, China). The Matrigel-embedded organoids were seeded as 25 μL droplets into pre-warmed 24-well plates and inverted in a CO_2 incubator at 37°C with 5% CO_2 for 20 min to allow complete gel solidification. Subsequently, 500 μL of pre-warmed GC organoid culture medium (Biorigin Biotechnology Co., Ltd., Beijing, China) was added to each well. Organoid morphology and growth were monitored by microscopy, and the culture medium was replaced every 3 – 5 days.

Sensitivity assay

When most organoids reached approximately 200 – 300 μm in diameter, they were collected and the original Matrigel was removed. The organoids were resuspended in fresh pre-chilled Matrigel at 1.5 times the original Matrigel volume. After thorough mixing, 7 μL of the Matrigel-organoid suspension was evenly dispensed onto the bottom of each well of a 96-well plate for subsequent organoid viability assessment. The seeded organoids were allowed to recover under standard culture conditions at 37°C with 5% CO_2. Drug treatment was initiated when most organoids reached approximately 100 – 200 μm in diameter as determined by microscopic observation. Specifically, the experimental group was treated with medium containing CHMs at the indicated concentrations, while GCOs treated with 0.1% DMSO served as the vehicle-control group. The 5-fluorouracil (5-FU)-treated group was used as the positive-control group. Each drug had six replicates, and the plates were incubated in the humidified CO_2 incubator at 37°C, 5% CO_2 for 5 – 7 days with fresh medium replaced halfway through the culture period. Organoid growth was monitored using XD inverted biological microscope (Ningbo Sunny Instruments Co., Ltd., Ningbo, Zhejiang, China). After 5 days of treatment, the plate and its contents were equilibrated to room temperature for about 30 min, after which 100 μL of CellTiter-Lumi™ reagent was added into each well. After shaking for 5 min to fully lyse the organoids, the plate was subjected to a 25-min incubation at room temperature in the dark to stabilize the luminescent signal. Luminescence intensity, which reflects intracellular ATP content, was measured using a multifunctional microplate reader according to the manufacturer's instructions. The luminescence signal was recorded as relative luminescence units (RLU). A curve was plotted and fitted to calculate the IC_{50} of each drug to assess the

vitality of GCOs. AnnexinV-FITC and 7-AAD flow cytometry were further used to analyze the different responses to the CHMs. Additionally, morphological changes in post-treatment GCOs were monitored using Olympus Provi CM20 real-time cell culture monitoring system (Olympus, Tokyo, Japan).

Western blot analysis

Western blotting was performed to assess the expression of apoptosis-related proteins from GCOs treated with ursolic acid at different concentrations of 0, 12.5, and 25 μM for 24 h. Total protein was extracted from the treated GCOs, and protein concentrations were determined using a BCA Protein Assay Kit (Beyotime Biotechnology Co., Ltd, Shanghai, China). Equal amounts of protein were separated by 10% SDS-PAGE and transferred onto PVDF membranes (Millipore, Billerica, MA, USA). The membranes were blocked with 5% non-fat milk at room temperature for 1.5 h and then incubated overnight at 4°C with primary antibodies against β-actin, PI3K, p-PI3K, AKT, p-AKT, P53, Bax, Bcl-2, cleaved caspase-3, and caspase-9 at the dilutions of β-actin (1:20,000), PI3K (1:1,000), p-PI3K (1:1,000), AKT (1:1,000), p-AKT (1:1,000), P53 (1:1,000), Bax (1:10,000), Bcl-2 (1:20,000), cleaved caspase-3 (1:20,000), and caspase-9 (1:1,000). After three times of washing with Tris-buffered saline containing Tween-20 (TBST), the membranes were incubated with horseradish peroxidase-conjugated secondary antibodies at 1:5,000, room temperature for 2 h. Protein bands were visualized using Amersham ImageQuant™ 800 chemiluminescence gel imaging system (Situofan Biotechnology Co., Ltd, Hangzhou, Zhejiang, China). Protein expression levels were quantified using Image Lab software (Bio-Rad, Philadelphia, PA, USA) with β-actin used as the internal loading control.

Statistical analysis

Data were presented as the mean ± standard deviation (SD). Statistical analyses were performed using SPSS Statistics software (version 18.0) (IBM Corp., Armonk, NY, USA). One-way analysis of variance was used to analyze the inter-group significance level. A significance level was set at $P < 0.05$.

Results and discussion

Screening of CHM-derived compounds with antiproliferative activity against GC cells

The antiproliferative effects of eight CHM-derived compounds demonstrated that all tested compounds inhibited cell proliferation in a time- and concentration-dependent manner, although the magnitude of inhibition varied among different compounds and cell lines. Curcumin, ursolic acid, erianin, and berberine exhibited relatively stronger antiproliferative activities compared with the other compounds ($P < 0.05$) (Figure 1). The IC_{50} values of each compound at 24, 48, and 72 h in the three GC cell lines were listed in Table 1. Consistent with the CCK-8 results, all eight CHM-derived compounds reduced the colony-forming ability of AGS, SGC-7901, and BGC-823 cells to varying degrees with more pronounced inhibition observed at higher concentrations. However, the inhibitory responses differed among the three GC cell lines, indicating cell line-dependent sensitivity to individual compounds. Notably, curcumin and berberine consistently suppressed colony formation in all three cell lines, while ursolic acid also exhibited significant inhibitory effects, particularly in AGS and SGC-7901 cells. The differential responses observed among GC cell lines might reflect the biological heterogeneity of GC and the distinct molecular characteristics affecting drug sensitivity. Based on the combined results from the CCK-8 and colony formation assays, curcumin, berberine, and ursolic acid were selected as the most promising candidates for subsequent validation in patient-derived GCOs. Previous studies have reported that curcumin inhibits GC cell proliferation through regulation of apoptosis-related pathways [18], while berberine exerts antiproliferative and apoptosis-inducing effects through modulation of NF-κB signaling [19]. Ursolic acid has also been shown to suppress GC cell growth in a time- and concentration-dependent manner [20]. These

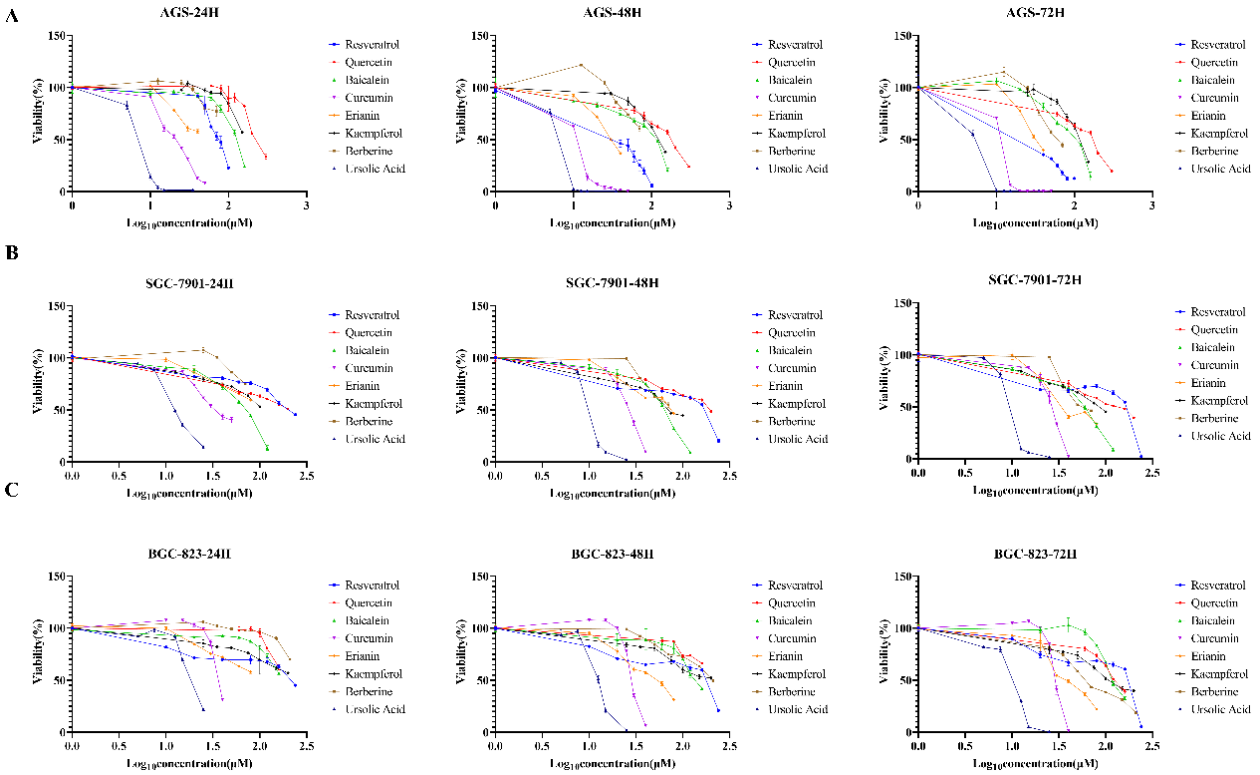


Figure 1. Screening of anti-proliferative effects of eight CHM-derived compounds on GC cells by CCK-8 assay. **A–C:** AGS, SGC-7901, and BGC-823 cells were treated with increasing concentrations of eight CHM-derived compounds for 24, 48, and 72 h.

Table 1. IC_{50} values of gastric cancer cell lines after treatments of 24, 48, and 72 h.

TCM	GC cell lines								
	AGS			SGC-7901			BGC-823		
	24 h	48 h	72 h	24 h	48 h	72 h	24 h	48 h	72 h
Curcumin (μM)	21.7	9.3	9.1	31.9	26.2	25.9	36.8	29.5	30.6
Berberine (μM)	112.3	78.4	55.0	92.2	69.3	48.5	263.4	212.2	68.4
Ursolic acid (μM)	7.4	6.1	4.7	12.6	10.3	10.0	20.2	12.1	10.1
Resveratrol (μM)	74.3	40.5	31.2	214.1	175.9	170.2	217.9	183.8	176.3
Quercetin (μM)	239.9	177.6	164.8	199.1	195.2	137.9	178.8	250.6	127.8
Erianin (nM)	43.0	30.1	30.7	105.0	75.8	40.3	98.1	50.2	39.7
Kaempferol (μM)	162.7	124.1	118.1	132.7	80.0	87.7	295.3	191.3	109.3
Baicalein (μM)	128.6	115.2	99.7	72.0	63.2	58.5	189.9	141.4	123.7

previous findings are consistent with the inhibitory effects observed in this study.

CHM-derived compounds induce apoptosis in GC cells

Annexin V–FITC/PI staining showed that treatment with the eight CHM-derived compounds significantly increased apoptosis in AGS, SGC-7901, and BGC-823 cells after 24 h with generally stronger effects observed at higher concentrations. The sensitivity of the three cell lines varied among the compounds. AGS cells were particularly responsive to curcumin, berberine, ursolic acid, resveratrol, and quercetin (Figure 2A), whereas SGC-7901 cells showed greater sensitivity to curcumin, berberine, and

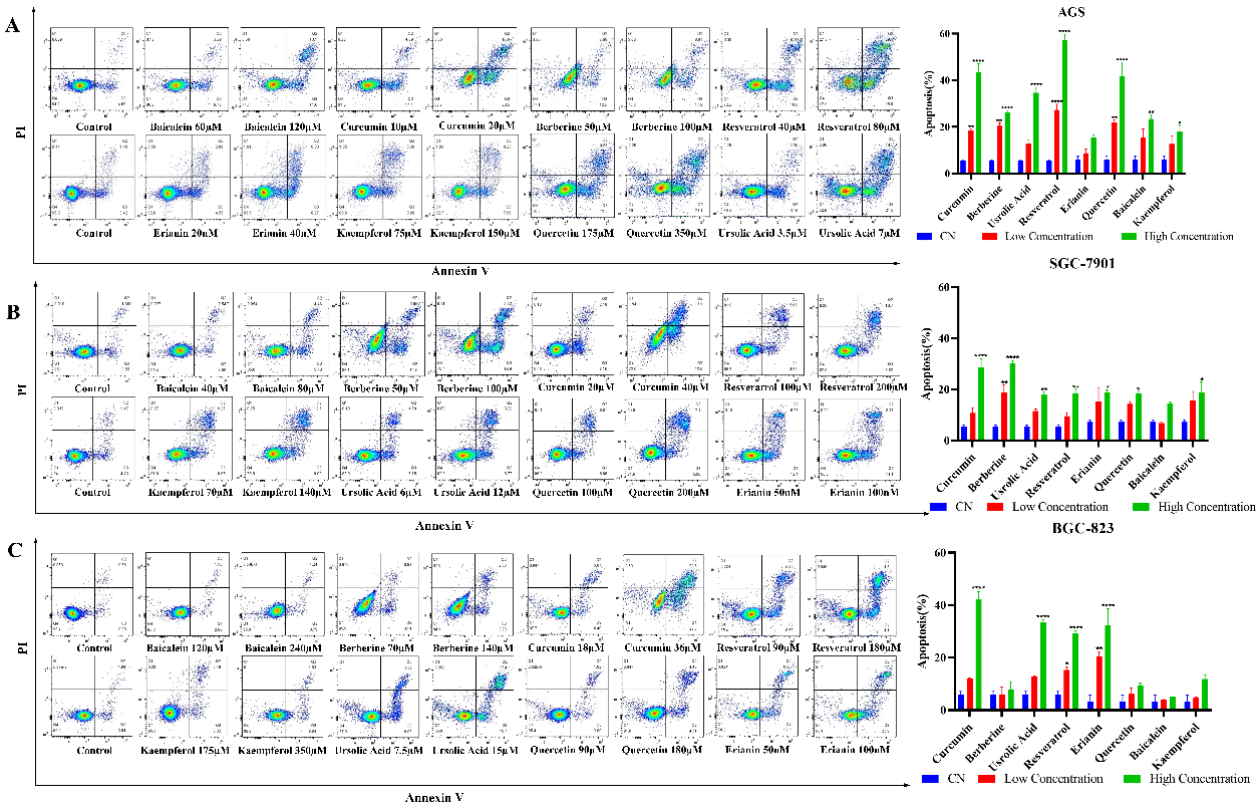


Figure 2. CHM-derived compounds induce apoptosis in GC cells. **A–C:** AGS, SGC-7901, and BGC-823 cells were treated with eight CHM-derived compounds at different concentrations for 24 h. *: $P < 0.01$. **: $P < 0.001$. ***: $P < 0.0001$.

ursolic acid (Figure 2B). BGC-823 cells were more sensitive to curcumin, ursolic acid, resveratrol, and erianin (Figure 2C). Curcumin, berberine, and ursolic acid induced apoptosis across all three GC cell lines. The increased apoptotic rates were consistent with the reduction in cell proliferation, suggesting that apoptosis induction contributed to the antitumor effects of these compounds. The distinct responses among the three cell lines further indicated that the efficacy of CHM-derived compounds might depend on cell-specific molecular characteristics. This heterogeneity highlighted the value of using multiple GC models to evaluate candidate antitumor compounds rather than relying on a single cell line [21]. Taken together, curcumin, berberine, and ursolic acid showed relatively consistent inhibitory and pro-apoptotic effects in GC cells and were therefore selected as candidate compounds for further validation using patient-derived GCOs.

Establishment and characterization of patient-derived GCO models

Patient-derived GCOs were successfully established from three GC samples and maintained under long-term culture conditions. The generated organoids exhibited heterogeneous morphological characteristics including solid and cystic-like structures among different patient-derived samples (Figure 3A). These differences indicated the diversity of organoid morphology among individual GC models. The established organoids could be continuously expanded through serial passaging for more than six months without obvious alterations in overall morphology (Figure 3B). Furthermore, organoids retained their structural characteristics after cryopreservation and subsequent recovery with no apparent morphological differences observed before freezing and after thawing (Figure 3C). The stable growth characteristics and long-term

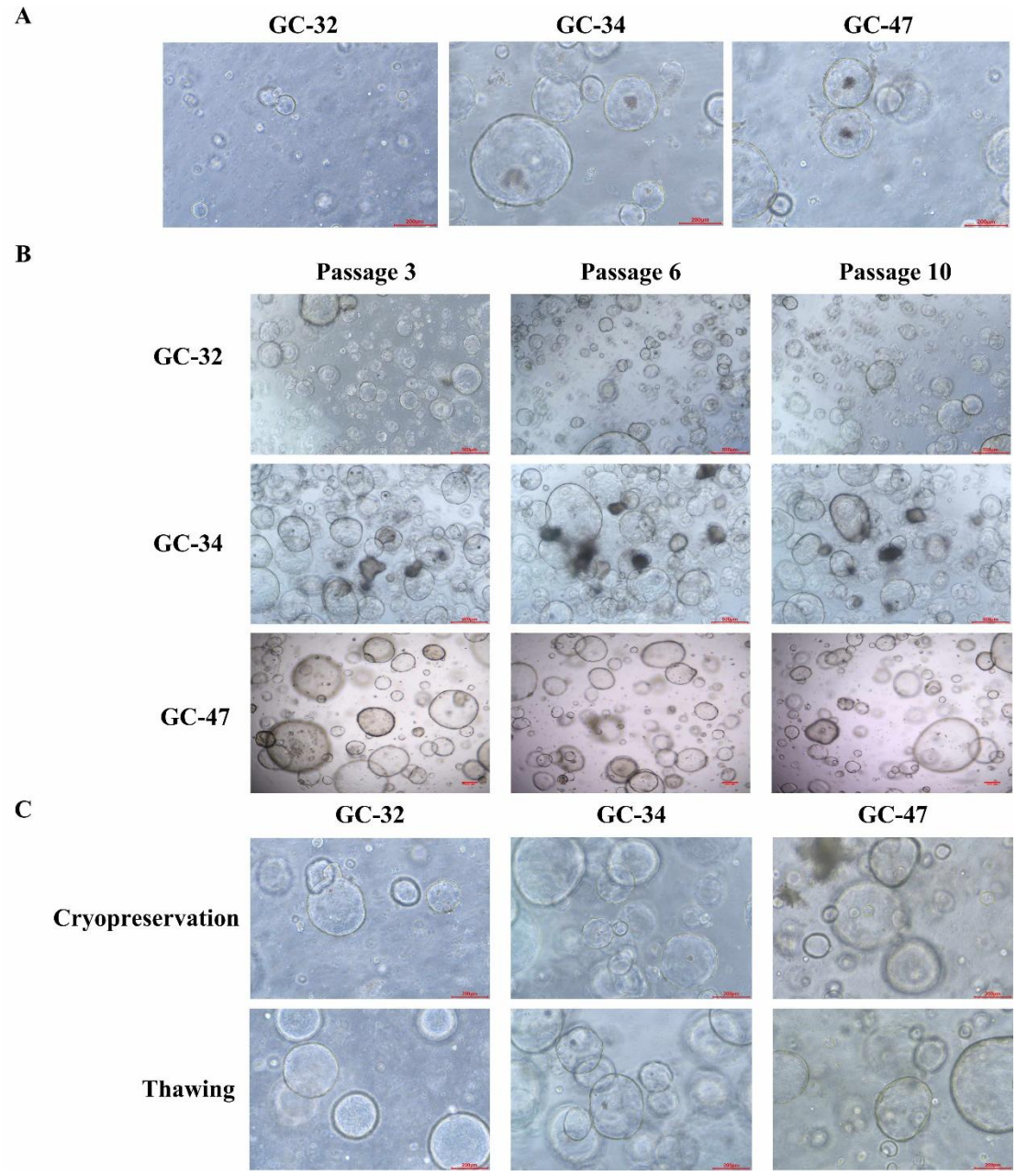


Figure 3. Establishment and characterization of patient-derived GCO models. **A.** Representative growth of successfully established GCOs (100×). **B.** After 5 – 6 days of culture, most organoids reached 200–300 µm in diameter with some exceeding 500 µm, enabling 1:2 or 1:3 passaging. GC-32 and GC-34 (40×) and GC-47 (100×). **C.** Morphology was preserved before cryopreservation and after thawing (100×).

maintainability of these patient-derived GCOs demonstrated their suitability as reproducible models for subsequent drug-response evaluation. Patient-derived tumor organoids retain important morphological and molecular features of the original tumors and could reflect interpatient and intratumoral heterogeneity [22, 23]. The observed morphological heterogeneity among different organoid lines might reflect the intrinsic differences between individual GC samples, highlighting the potential of patient-derived organoids for evaluating heterogeneous responses to anticancer compounds.

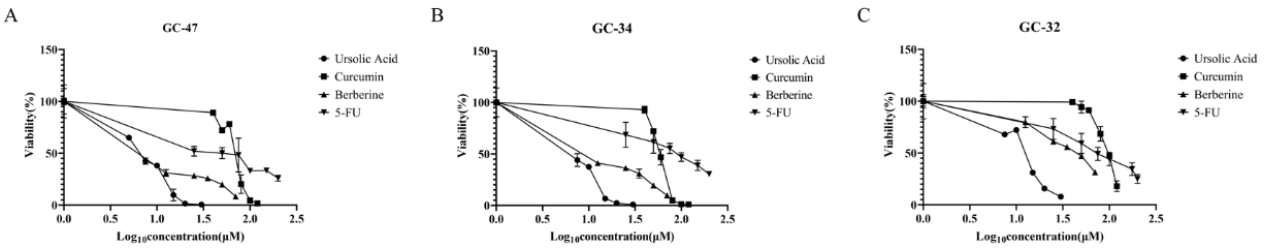


Figure 4. Drug sensitivity of patient-derived GCOs to selected CHM-derived compounds. **A–C:** GC-32, GC-34, and GC-47 organoids were treated with curcumin, berberine, ursolic acid, and 5-fluorouracil (5-FU) for 120 h.

Selected CHM-derived compounds inhibit the viability of patient-derived GCOs

Following the screening results obtained from GC cell models, curcumin, berberine, and ursolic acid were further evaluated using patient-derived GCOs (GC-32, GC-34, and GC-47) to determine whether their inhibitory effects could be reproduced in a clinically relevant three-dimensional model. Quantitative viability analysis revealed significant differences in the IC_{50} values of different compounds within the same organoid line, as well as differences in the response of different organoid lines to the same compound (Table 2). After 120 h of treatment, ursolic acid, berberine, and curcumin showed a broadly consistent inhibitory trend across the three GCO lines (Figure 4). Among the tested compounds, ursolic acid and berberine generally exhibited stronger inhibitory effects than curcumin with lower IC_{50} values observed in most organoid models. Compared with 5-fluorouracil (5-FU), several organoid lines showed greater sensitivity to ursolic acid and berberine under the present experimental conditions. The inhibitory effects observed in the organoid models were generally consistent with those obtained in the GC cell lines. However, the magnitude of the responses differed among GC-32, GC-34, and GC-47, highlighting the influence of interpatient heterogeneity on drug sensitivity. GCOs established from different patients could therefore provide complementary information that might not be captured by conventional two-dimensional cell models. Previous studies have established organoid libraries from gastric and colorectal cancers as preclinical platforms for drug screening [24]. The present findings further supported the potential utility of patient-derived GCOs for evaluating individual responses to CHM-derived compounds.

Table 2. IC_{50} values of gastric cancer organoids after 120 h of treatment.

Drug name	Organoid ID	IC_{50} (μM)
Curcumin	GC-32	96.910 ± 3.590
	GC-34	60.516 ± 0.550
	GC-47	66.634 ± 1.347
Berberine	GC-32	44.916 ± 1.201
	GC-34	13.127 ± 0.220
	GC-47	10.523 ± 0.340
Ursolic acid	GC-32	13.408 ± 1.003
	GC-34	6.796 ± 0.210
	GC-47	7.062 ± 0.195
5-FU	GC-32	81.446 ± 7.446
	GC-34	76.696 ± 6.577
	GC-47	40.801 ± 2.648

CHMs induce apoptosis in patient-derived GCOs

Following the evaluation of growth inhibition, the pro-apoptotic effects of curcumin, berberine, and ursolic acid were further investigated in patient-derived GCOs (GC-32, GC-34, and GC-47). Compared with the control groups, all three compounds significantly increased apoptotic rates in GCOs (Figure 5). However, the extent of apoptosis induction varied among different organoid lines and compounds, indicating heterogeneous responses among patient-derived models. GC-32 showed a strong apoptotic response to berberine treatment, particularly at higher concentration, whereas GC-34 exhibited greater sensitivity to curcumin. GC-

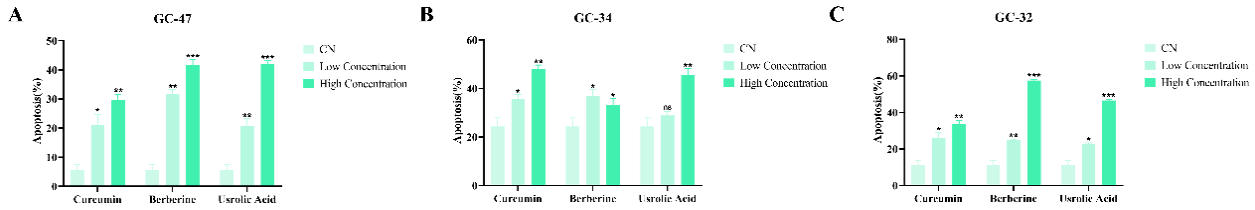


Figure 5. CHM-derived compounds induce apoptosis in patient-derived GCOs. **A–C:** GC-32, GC-34, and GC-47 organoids were treated with curcumin, berberine, or ursolic acid at different concentrations. *: $P < 0.01$. **: $P < 0.001$. ***: $P < 0.0001$.

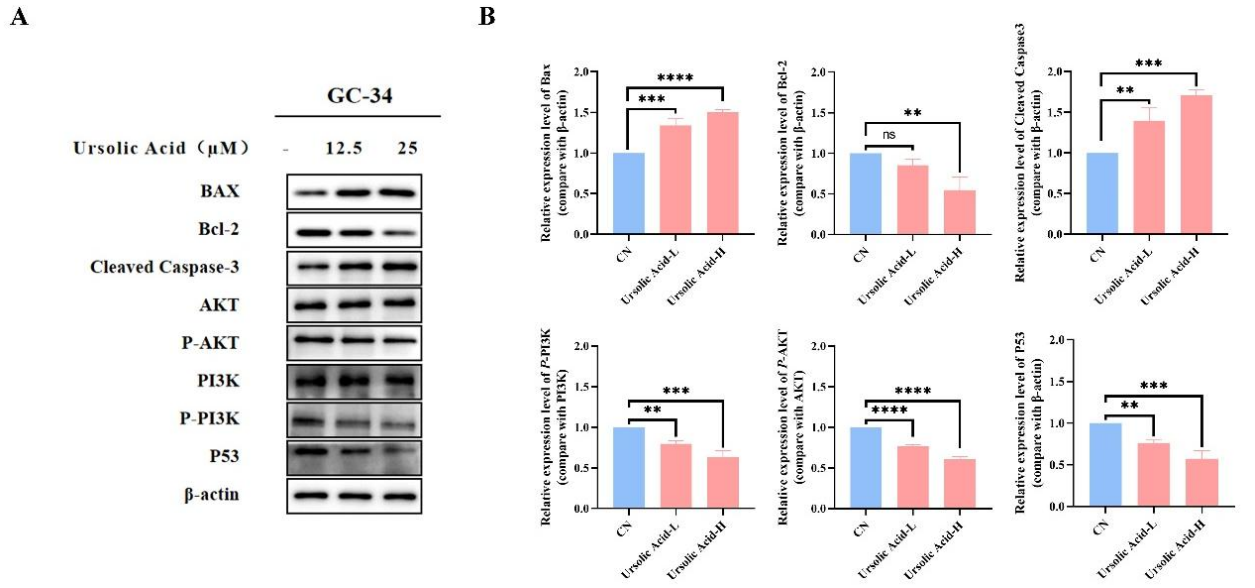


Figure 6. Effect of ursolic acid on apoptosis and AKT/PI3K signaling pathway in GCOs. **A.** 24 h treatment with ursolic acid at high (25 μM) and low (12.5 μM) doses. **B.** Relative expression levels of Bax, Cleaved Caspase-3, Bcl-2, p-PI3K, p-AKT/Akt, and P53 in gastric cancer organoids. ns: not significant. *: $P < 0.01$. **: $P < 0.001$. ***: $P < 0.0001$.

47 organoids showed a pronounced apoptotic response following ursolic acid treatment. Although concentration-dependent increases in apoptosis were observed in several treatment groups, some organoid lines displayed compound-specific response patterns, suggesting that drug sensitivity might depend on the biological characteristics of individual tumors. The increased apoptotic rate was consistent with the reduction in organoid viability observed in the growth inhibition assay, indicating that apoptosis induction contributed to the inhibitory effects of curcumin, berberine, and ursolic acid on GCOs. The heterogeneous apoptotic responses among different patient-derived organoid lines further demonstrated the potential value of organoid models for evaluating individualized responses to anticancer compounds.

Ursolic acid modulates apoptosis-related proteins and PI3K/Akt signaling in GCOs

Western blot analysis showed that, compared with the control group, ursolic acid significantly increased the expression of Bax and cleaved caspase-3 and decreased the expression of Bcl-2 (Figure 6). In addition, the levels of p-PI3K and p-AKT were significantly reduced following ursolic acid treatment. Changes in P53 expression were also observed in the treated organoids. In addition, ursolic acid treatment reduced the phosphorylation levels of PI3K and AKT, whereas

total PI3K and AKT expression showed no obvious changes. These results suggested that ursolic acid might suppress PI3K/AKT pathway activation in GCOs. Changes in P53 expression were also observed after ursolic acid treatment. However, the functional significance of this alteration required further investigation due to the complex and context-dependent role of P53 in GC. Bcl-2 family proteins and caspases are key regulators of the mitochondrial apoptotic pathway [25, 26]. The increased Bax and cleaved caspase-3 levels together with decreased Bcl-2 expression supported the involvement of mitochondrial apoptosis in ursolic acid-induced inhibition of GC-34 organoid growth. The reduction in phosphorylated PI3K and AKT further indicated that suppression of PI3K/AKT signaling might contribute to the pro-apoptotic effects of ursolic acid. These findings were consistent with previous reports describing the antitumor activity of ursolic acid in GC models [18]. However, the present study demonstrated an association between ursolic acid treatment, PI3K/AKT signaling alteration, and apoptosis induction, and additional pathway-specific intervention experiments were required to confirm a direct causal relationship.

Limitations

Although the present study demonstrated inhibitory and pro-apoptotic effects of selected CHM-derived compounds in GC cell lines and patient-derived organoids, several limitations should be considered. This study only included three patient-derived organoid lines, which might not represent the full molecular and clinical heterogeneity of GC. Further, the findings were obtained primarily from *in vitro* experiments, and the bioavailability, systemic toxicity, pharmacokinetics, and therapeutic efficacy of these compounds remained to be evaluated *in vivo*. Furthermore, the involvement of the PI3K/Akt pathway was inferred from changes in protein expression and phosphorylation, and further functional validation was required. Future studies using larger organoid cohorts, patient-derived organoid xenograft models, and pathway-specific intervention experiments would be necessary to confirm these findings and assess their translational relevance.

Conclusion

This study systematically evaluated the differential inhibitory effects of eight CHMs on the proliferation of three GC cell lines with the identification of curcumin, berberine, and ursolic acid as the most promising drug candidates. Ursolic acid was further validated to have significantly stronger ability of inducing cell apoptosis in organoids than in cell lines, suggesting that it might target tumor microenvironment dependence mechanisms. Mechanistically, ursolic acid induced GC cell apoptosis by inactivating the PI3K/Akt pathway.

Acknowledgements

This work was supported by the National Natural Science Foundation of China (Grant No. 31100499) and the Key Research & Development Program of Zhejiang Province (Grant No. 2024C03075).

References

1. Sexton RE, Al-Hallak MN, Diab M, Azmi AS. 2020. Gastric cancer: A comprehensive review of current and future treatment strategies. Cancer Metast Rev. 39(4):1179-1203.
2. Thrift AP, El-Serag HB. 2020. Burden of gastric cancer. Clin Gastroenterol H. 18(3):534-524.
3. Yusefi A, Bagheri L, Bastani P, Radinmanesh M, Kavosi Z. 2018. Risk factors for gastric cancer: A systematic review. Asian Pac J Cancer P. 19(3):591-603.
4. Praud D, Rota M, Pelucchi C, Bertuccio P, Rosso T, Galeone C, *et al*. 2018. Cigarette smoking and gastric cancer in the Stomach Cancer Pooling (StoP) Project. Eur J Cancer Prev. 27(2):124-133.
5. Ford AC, Yuan Y, Moayyedi P. 2020. *Helicobacter pylori* eradication therapy to prevent gastric cancer: Systematic review and meta-analysis. Gut. 69(12):2113-2121.
6. Du X, Yan Y, Liu B. 2022. Updated interpretation of the 2022 Chinese Society of Clinical Oncology (CSCO) guidelines for gastric cancer diagnosis and treatment. J Clin Surg. 30(9):805-808.

7. Yao CL, Zhang JQ, Li JY, Wei WL, Wu Sf, Guo DA. 2021. Traditional Chinese medicine (TCM) as a source of new anticancer drugs. Nat Prod Rep. 38(9):1618-1633.
8. Cheng MQ, Hu JQ, Zhao YW, Jiang JL, Qi RZ, Chen ST, *et al*. 2021. Efficacy and safety of *Astragalus*-containing Traditional Chinese Medicine combined with platinum-based chemotherapy in advanced gastric cancer: A systematic review and meta-analysis. Front Oncol. 11:632168.
9. Bu ZJ, Wan SR, Steinmann P, Yin ZT, Tan JP, Li WX, *et al*. 2024. Effectiveness and safety of Chinese herbal injections combined with SOX chemotherapy regimens for advanced gastric cancer: A Bayesian network meta-analysis. J Cancer. 15(4):889-907.
10. Liu YY, Yu XF, Shen HZ, Hong YJ, Hu GF, Niu WY, *et al*. 2024. Mechanisms of traditional Chinese medicine in the treatment and prevention of gastric cancer. Phytomedicine. 135:156003.
11. Xu J, Yu BX, Wang F, Yang J. 2024. Xenograft and organoid models in developing precision medicine for gastric cancer (Review). Int J Oncol. 64(4):41.
12. Foglietta F, Canaparo R, Muccioli G, Terreno E, Serpe L. 2020. Methodological aspects and pharmacological applications of three-dimensional cancer cell cultures and organoids. Life Sci. 254:117784.
13. Kondo J, Inoue M. 2019. Application of cancer organoid model for drug screening and personalized therapy. Cells. 8(5):470.
14. Kiyohara Y, Yoshino K, Kubota S, Okuyama H, Endo H, Ueda Y, *et al*. 2016. Drug screening and grouping by sensitivity with a panel of primary cultured cancer spheroids derived from endometrial cancer. Cancer Sci. 107(4):452-460.
15. Steele NG, Chakrabarti J, Wang J, Biesiada J, Holokai L, Chang J, *et al*. 2019. An organoid-based preclinical model of human gastric cancer. Cell Mol Gastroenterol Hepatol. 7(1):161-184.
16. Seidlitz T, Merker SR, Rothe A, Zakrzewski F, Neubeck CV, Grützmann K, *et al*. 2019. Human gastric cancer modelling using organoids. Gut. 68(2):207-217.
17. Liao YL, Gui Y, Li QZ, An J, Wang D. 2023. The signaling pathways and targets of natural products from traditional Chinese medicine treating gastric cancer provide new candidate therapeutic strategies. Biochim Biophys Acta Rev Cancer. 1878(6):188998.
18. Sun QQ, Zhang WJ, Guo YJ, Li ZY, Chen XN, Wang YY, *et al*. 2016. Curcumin inhibits cell growth and induces cell apoptosis through upregulation of miR-33b in gastric cancer. Tumor Biol. 37(10):13177-13184.
19. Pandey MK, Sung B, Kunnumakkara AB, Sethi G, Chaturvedi MM, Aggarwal BB. 2008. Berberine modifies cysteine 179 of IκBα kinase, suppresses nuclear factor-κB-regulated antiapoptotic gene products, and potentiates apoptosis. Cancer Res. 68(13):5370-5379.
20. Wang XM, Zhang F, Yang L, Mei Y, Long H, Zhang XW, *et al*. 2011. Ursolic acid inhibits proliferation and induces apoptosis of cancer cells *in vitro* and *in vivo*. J Biomed Biotechnol. 2011:419343.
21. Choong ML, Tan SH, Tan TZ, Manesh S, Ngo A, Yong JW, *et al*. 2014. Molecular integrative clustering of Asian gastric cell lines revealed two distinct chemosensitivity clusters. PLoS One. 9(10):e111146.
22. Kopper O, Witte CJ, Lohmussaar K, Valle-Inclan JE, Hami N, Kester L, *et al*. 2019. An organoid platform for ovarian cancer captures intra- and interpatient heterogeneity. Nat Med. 25(5):838-849.
23. Lo YH, Karlsson K, Kuo CJ. 2020. Applications of organoids for cancer biology and precision medicine. Nat Cancer. 1(8):761-773.
24. Fujii M, Shimokawa M, Date S, Takano A, Matano M, Nanki K, *et al*. 2016. A colorectal tumor organoid library demonstrates progressive loss of niche factor requirements during tumorigenesis. Cell Stem Cell. 18(6):827-838.
25. Lv D, Liu YL, Tang RY, Fu S, Kong SS, Liao Q, *et al*. 2024. Analysis of clinical trials using anti-tumor Traditional Chinese Medicine monomers. Drug Des Devel Ther. 18:1997-2020.
26. Xu HL, Zhao X, Liu XH, Xu PX, Zhang KM, Lin XK. 2015. Antitumor effects of traditional Chinese medicine targeting the cellular apoptotic pathway. Drug Des Devel Ther. 9:2735-2744.